

### Unitary states for three pions\*†

G. Ascoli and H. W. Wyld

Department of Physics, University of Illinois, Urbana, Illinois 61801

(Received 26 February 1975)

Recent angular momentum analyses of the three-pion system produced in the reaction  $\pi^-p \rightarrow \pi^- \pi^+ \pi^- p$  have been criticized because the three-pion states used in the analysis do not satisfy unitarity. In order to answer this criticism we develop a set of unitarity equations which can be solved to yield a set of three-pion states which explicitly satisfy both three-particle unitarity and two-particle unitarity (Watson's theorem). A numerical method for solving the equations is given. When the unitary states are used to reanalyze the data for the reaction  $\pi^-p \rightarrow \pi^- \pi^+ \pi^- p$  we find some changes in the detailed numerical fits but no change in the general conclusions. In particular, the phase of the amplitude for the  $A_1$  state varies only slightly in the  $A_1$  mass region, in contrast with the behavior expected for a resonant state.

#### I. INTRODUCTION

In the past four years a large-scale effort<sup>1-9</sup> has been made to perform a complete angular momentum analysis for the three-pion system produced in the reaction

$$\pi^- p \rightarrow \pi^- \pi^+ \pi^- p. \tag{1.1}$$

We can recapitulate some of the major points of this analysis here. The distribution in angles and energies of the three pions on the right-hand side of reaction (1.1) is described by a formula of the type

$$\sum_{JMP} \sum_{J'M'P'} \mathfrak{M}_{J'M'P',JMP} \rho_{J'M'P',JMP} \mathfrak{M}_{JMP}^*. \tag{1.2}$$

Here  $\rho_{J'M'P',JMP}$  is a density matrix describing the production of a state with quantum numbers  $J$ =total angular momentum,  $M$ = $z$  projection of angular momentum, and  $P$ =parity.

The matrix element  $\mathfrak{M}_{JMP}$  describes the decay of this state into three pions. In order to write down an explicit formula for  $\mathfrak{M}_{JMP}$  we shall work in the center-of-mass system of coordinates for the three pions with the  $z$  axis along the direction of motion of the incoming pion as viewed in this system. The three-pion states can be described in the old Dalitz terminology of a pion 1 plus a dipion 23. We take particle 3 to be the  $\pi^+$  and particles 1 and 2 to be the  $\pi^-$ 's. The Bose symmetry will be taken account of by symmetrizing  $1 \leftrightarrow 2$ . The analysis of the experimental data was performed in terms of Dalitz-plot variables ( $s_1, s_2$ ) and Euler angles ( $\alpha, \beta, \gamma$ ) describing the orientation of the three-pion system—see Refs. 1 and 5 for details. For our purposes here it is more convenient to use the mass of the dipion  $\sqrt{s_1}$  and two sets of polar and azimuthal angles. The relation

between these different sets of variables is given in Appendix A. The four angles necessary are illustrated in Fig. 1;  $\Omega_1 = (\theta_1, \varphi_1)$  are the polar and azimuthal angles locating the dipion 23 in the three-pion center-of-mass system, and  $\bar{\Omega}_1 = (\bar{\theta}_1, \bar{\varphi}_1)$  are the polar and azimuthal angles locating pion 3, the  $\pi^+$ , in the dipion center-of-mass system relative to the same set of axes. An appropriate complete set of angular momentum states for the three-pion system is the set of functions

$$Z_{LS}^{JM}(\Omega_1, \bar{\Omega}_1) = \sum_{M_L, M_S} \langle JM | LSM_L M_S \rangle Y_{L^M}^{M_L}(\Omega_1) Y_S^{M_S}(\bar{\Omega}_1). \tag{1.3}$$

Here  $S$  is the angular momentum of the dipion 23 and  $L$  is the orbital angular momentum of the dipion relative to the other pion 1. The spherical

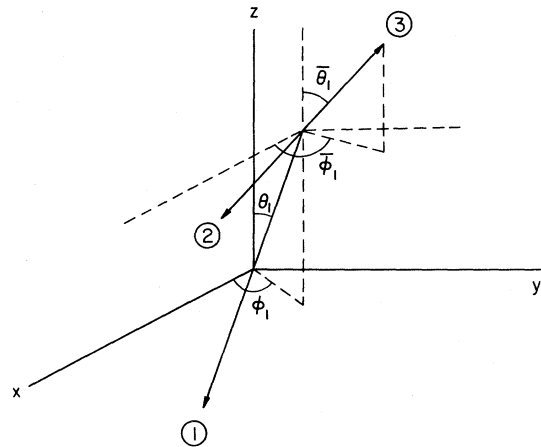


FIG. 1. Angular coordinates used to describe the orientation of the three pions.

harmonics are coupled with a Clebsch-Gordan coefficient  $\langle JM | LSM_L M_S \rangle$  to obtain a state of total angular momentum  $J$  and  $z$  projection  $M$ . If instead of 23 as the dipion we take 13 as the dipion we will have a different set of angles  $\Omega_2 = (\theta_2, \varphi_2)$ ,  $\bar{\Omega}_2 = (\bar{\theta}_2, \bar{\varphi}_2)$  and a different complete set of angular momentum states  $Z_{LS}^{JM}(\Omega_1, \bar{\Omega}_1) \leftrightarrow Z_{LS}^{JM}(\Omega_2, \bar{\Omega}_2)$ .

What has been said so far is unexceptionable.

Some plausible but not completely general assumptions are now made about the matrix element  $\mathfrak{M}_{JMP}$  for the decay of the state with quantum numbers  $JMP$ :

$$\mathfrak{M}_{JMP} = \sum_{L,S} C_{LS}^J(W) \mathfrak{M}_{LS}^{JMP}, \quad (1.4a)$$

$$\mathfrak{M}_{LS}^{JMP} = \mathfrak{R}_{LS}(s_1, W) Z_{LS}^{JM}(\Omega_1, \bar{\Omega}_1) + (1 \leftrightarrow 2). \quad (1.4b)$$

Thus, it is assumed that  $\mathfrak{M}_{JMP}$  can be written in a suitably Bose-symmetrized factorizable product form.  $C_{LS}^J(W)$  is independent of  $M$  and is a function only of the three-pion invariant mass  $W$ ,

$$W^2 = (p_1 + p_2 + p_3)^2. \quad (1.5)$$

$\mathfrak{R}_{LS}(s_1, W)$  is independent of  $J$  and  $M$  and is a function of  $W$  and the dipion mass  $\sqrt{s_1}$ ,

$$s_1 = (p_2 + p_3)^2. \quad (1.6)$$

As written in Eq. (1.4) it is assumed that the state with quantum numbers  $JMP$  decays coherently (like a resonant state with these quantum numbers). This assumption can be eliminated by treating the states with different  $L, S$  separately, i.e., by transferring the  $\sum_{L,S}$  in (1.4) to (1.2) and using an enlarged density matrix  $\rho_{JMPLS, J'M'P'L'S'}$ .

In practice  $L$  and  $S$  are restricted to low values  $S = 0, 1, 2$ ,  $L = 0, 1, 2, 3$ , and a Breit-Wigner form with appropriate threshold factors is used for  $\mathfrak{R}_{LS}(s_1, W)$ :

$$\mathfrak{R}_{LS}(s_1, W) = \frac{p_1^L q_1^S}{M_R^2 - s_1 - iM_R \Gamma}, \quad (1.7)$$

$$\Gamma = \Gamma_R \left( \frac{q_1}{q_R} \right)^{2S+1} \frac{M_R}{\sqrt{s_1}}. \quad (1.8)$$

Here  $p_1$  is the relative momentum in the pion 1 + dipion 23 system,

$$p_1 = \frac{1}{2W} \{ [W^2 - (\sqrt{s_1} - m_\pi)^2] [W^2 - (\sqrt{s_1} + m_\pi)^2] \}^{1/2}, \quad (1.9)$$

$q_1$  is the relative momentum in the dipion 23 system,

$$q_1 = \frac{1}{2}(s_1 - 4m_\pi^2)^{1/2}, \quad (1.10)$$

and  $M_R$  and  $\Gamma_R$  are the mass and width of one or the other of the three well-known dipion resonances (see Table I).  $q_R$  in (1.8) is  $q_1$  [(1.10)] evaluated

TABLE I. Resonance parameters employed in Eq. (1.7).

|            | $M_R$ (GeV) | $\Gamma_R$ (GeV) |
|------------|-------------|------------------|
| $\epsilon$ | 0.765       | 0.400            |
| $\rho$     | 0.765       | 0.135            |
| $f$        | 1.269       | 0.154            |

at  $s_1 = M_R^2$ . The formula (1.7) corresponds to a cascade decay process. The system first decays into a pion plus a dipion resonance of spin  $S$ . The Breit-Wigner denominator describes the propagation of the resonant state. Finally the dipion resonance decays into two pions. The threshold factors in the numerator are the simplest possible approximations to the matrix elements for the successive two-particle decay processes.

The angular momentum analysis of the experimental data for the reaction (1) is performed by fitting the data with the functions described above using a maximum-likelihood method.<sup>1,5</sup> The fitting procedure determines the density-matrix elements  $\rho_{JMP, J'M'P'}$  [(1.2)] and the parameters  $C_{LS}^J(W)$  which appear in (1.4), or at least bilinear combinations  $C_{LS}^J(W) C_{L'S'}^{J'}(W)^*$  of them.

When the analysis was performed some unexpected and puzzling features appeared.<sup>2,5,7,9</sup> It was found, for example, that the absolute magnitude of the amplitude  $C_{01}^1$  corresponding to the  $L=0, S=1$  ( $\rho\pi$  S-wave) component of the  $J^P = 1^+$  state had a nice Breit-Wigner-shaped bump as a function of the three-pion mass  $W$ , corresponding to the  $A_1$  meson. However, the phase of this state turned out to be nearly constant (relative to the phases of several other states where no resonant behavior was detected). If the  $A_1$  is a true meson, one would expect the characteristic Breit-Wigner variation of phase. A similar behavior was found for the  $A_{3,5}$ , a peak in the magnitude of the  $L=0, S=2$  ( $f\pi$  S-wave) amplitude with no corresponding phase variation. The  $A_2$  peak, on the other hand, behaved in a normal fashion,<sup>4</sup> both magnitude and phase exhibiting the characteristic Breit-Wigner variation. Another puzzling feature was the relative phase difference of  $90^\circ$  found between the  $L=0, S=1$  ( $\rho\pi$  S-wave) and  $L=1, S=0$  ( $\epsilon\pi$  P-wave) contributions to the  $J^P = 1^+ A_1$  peak. One might expect these two contributions to be relatively real.

Since these results were puzzling and since they contradict the generally successful quark model in which the  $A_1$  is a perfectly well-defined resonant state, criticism<sup>10</sup> has been made of the procedure for analysis described above, in particular of the structure of Eqs. (1.4) and (1.7). Perhaps some error has been introduced, because the three-pion states described by (1.4) and (1.7) do not satisfy

either three-particle or two-particle unitarity.

In this paper we attempt to answer this criticism by developing a set of unitarity equations which can be solved to yield a set of three-pion states which explicitly satisfy both three-particle unitarity and two-particle unitarity. In Sec. II we write down the three-particle unitarity equations in the form of a Heitler equation relating the  $T$  matrix for three-particle scattering to a real  $K$  matrix. The  $K$  matrix is then chosen as the form corresponding to Eqs. (1.4) and (1.7) above. The solutions of the resulting Faddeev-type integral equations yield the simplest possible unitary generalization of (1.4) and (1.7). In Sec. III the threshold behavior of the equations is discussed and it is shown that two-particle unitarity (Watson's theorem) is also satisfied. In Sec. IV a numerical procedure for solving the integral equations is discussed and some results are displayed for a typical case. In Sec. V we discuss what differences appeared relative to the original nonunitary analysis when the

experimental data were reanalyzed with the unitary three-pion states. Two appendixes are devoted to the recoupling operators for orbital and isospin states used in the integral equations. A preliminary account of this work has already appeared.<sup>11</sup>

## H. THREE-PARTICLE UNITARITY

The  $S$  matrix for three-particle  $\rightarrow$  three-particle scattering can be written in terms of a Lorentz-invariant  $T$  matrix as

$$S_{ij} = \delta_{ij} + i(2\pi)^4 \delta^4(P_{i_1} + P_{i_2} + P_{i_3} - P_{j_1} - P_{j_2} - P_{j_3}) \times \frac{T_{ij}}{(2^6 \omega_{i_1} \omega_{i_2} \omega_{i_3} \omega_{j_1} \omega_{j_2} \omega_{j_3})^{1/2}}. \quad (2.1)$$

Elastic unitarity for the  $S$  matrix,

$$\sum_k S_{ik} S_{jk}^* = \delta_{ij}, \quad (2.2)$$

then yields for the  $T$  matrix the relation

$$\begin{aligned} \text{Im} T_{ij} &= \frac{1}{2i} (T_{ij} - T_{ji}^*) \\ &= \frac{(2\pi)^4}{2} \sum_k \frac{T_{ik} T_{jk}^*}{8 \omega_{k_1} \omega_{k_2} \omega_{k_3}} \delta^4(P_{i_1} + P_{i_2} + P_{i_3} - P_{k_1} - P_{k_2} - P_{k_3}), \end{aligned} \quad (2.3)$$

where we have also used the symmetry of the  $T$  matrix,  $T_{ij} = T_{ji}$ , which follows from parity conservation and time-reversal invariance. In Eq. (2.3) the summation over intermediate states  $k$  involves three-particle phase space and can be written in the following way:

$$\begin{aligned} \sum_k \frac{\delta^4(P - P_{k_1} - P_{k_2} - P_{k_3})}{8 \omega_{k_1} \omega_{k_2} \omega_{k_3}} \dots &= \frac{1}{(2\pi)^9} \int \delta^4(P - P_{k_1} - P_{k_2} - P_{k_3}) \frac{d^3 P_{k_1}}{2 \omega_{k_1}} \frac{d^3 P_{k_2}}{2 \omega_{k_2}} \frac{d^3 P_{k_3}}{2 \omega_{k_3}} \dots \\ &= \frac{1}{8(2\pi)^9 W} \int d\Omega_1 d\bar{\Omega}_1 d(\sqrt{s_1}) p_1 q_1 \dots \end{aligned} \quad (2.4)$$

The kinematic variables in the last line of (2.4) have all been defined in the Introduction and in Fig. 1.

The  $T$  matrix discussed above describes a transition with three particles in the initial state and three particles in the final state. We can describe both the initial and the final states with the pion 1 + dipion 23 set of variables introduced in the Introduction. Suppose the initial state is described by variables  $s_1, \Omega_1, \bar{\Omega}_1$  and the final state by variables  $s'_1, \Omega'_1, \bar{\Omega}'_1$ . From rotational invariance it follows that the 3-3  $T$  matrix can be expanded as

$$\begin{aligned} T &= \sum_J \sum_{LS} \sum_{L'S'} T_{L'S', LS}^J(s'_1, s_1) \\ &\quad \times \sum_M Z_{L'S'}^{JM}(\Omega'_1, \bar{\Omega}'_1) Z_{LS}^{JM*}(\Omega_1, \bar{\Omega}_1), \end{aligned} \quad (2.5)$$

where the angular momentum functions  $Z_{LS}^{JM}$  are given in Eq. (1.3). Substituting (2.5) and (2.4) in (2.3) and using the orthogonality properties of the  $Z_{LS}^{JM}$ , we find the angular momentum decomposition of the unitarity relation,

$$\begin{aligned} \text{Im} T_{L'S', LS}^J(s'_1, s_1) &= \sum_{L''S''} \int d((s''_1)^{1/2}) T_{L'S', L''S''}^J(s'_1, s''_1) \\ &\quad \times \rho T_{LS, L''S''}^{J*}(s_1, s''_1), \end{aligned} \quad (2.6)$$

where

$$\rho = \frac{2}{(4\pi)^5} \frac{p_1'' q_1''}{W}. \quad (2.7)$$

We note in passing that  $\rho$  is uniquely determined by the relativistic kinematics. There is no ambiguity of the sort encountered in trying to write down the propagators for a relativistic three-particle

Schrödinger equation.

We can ensure that (2.6) is satisfied by introducing a suitable real  $K$  matrix. The argument is essentially the same as in the two-particle case. (We apologize for writing down for the sake of the nonexpert all these things so well known to experts on the three-particle problem.) Write (2.6) in an abbreviated notation as

$$\text{Im}T = \frac{1}{2i} (T - T^\dagger) = T\rho T^\dagger, \quad (2.8)$$

where

$$T = T_{L'S',LS}^J(s'_1, s_1) = T_{LS,L'S'}^J(s_1, s'_1) \quad (2.9)$$

$$T_{L'S',LS}^J(s'_1, s_1) = K_{L'S',LS}^J(s'_1, s_1) + i \sum_{L''S''} \int_{2m\pi}^{W-m\pi} d((s_1'')^{1/2}) K_{L'S',L''S''}^J(s'_1, s_1'') \rho T_{L''S'',LS}^J(s_1'', s_1), \quad (2.13)$$

with  $\rho$  again given by (2.7).

As long as  $K$  is chosen to be a real symmetric matrix, the  $T$  which results from solving (2.13) will be a symmetric matrix satisfying the three-particle unitarity relation (2.6). In order to obtain the simplest possible generalization of the scheme described in the Introduction, Eqs. (1.4) and (1.7), we shall take  $K$  to be the sum of three terms, each of these being a two-particle  $K$  matrix with the third particle a spectator:

$$K = k_1 + k_2 + k_3. \quad (2.14)$$

This is illustrated in Fig. 2. Note that  $k_1$ ,  $k_2$ ,  $k_3$  represent the interactions of the particle pairs 23, 13, and 12, respectively. We hasten to add that the assumed form of (2.14) as the sum of three two-body terms is an approximation. An exact expression for  $K$  would include in addition to the terms in (2.14) other "connected" terms which cannot be separated into a two-body interaction with the third particle a spectator. For example, a three-particle resonance would be described by a connected term of this sort. We do not include such three-particle resonance terms here, be-

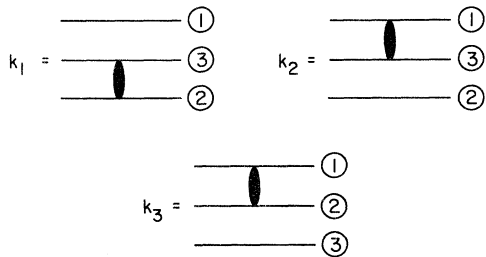


FIG. 2. Graphs corresponding to the assumption (2.14) for the  $K$  matrix.

is a symmetric matrix with one continuous index and  $\rho$  is a diagonal matrix. Rewriting (2.8) in the form

$$(T^\dagger)^{-1} - T^{-1} = 2i\rho, \quad (2.10)$$

we see that if we define the  $K$  matrix by

$$T^{-1} = K^{-1} - i\rho \quad (2.11)$$

then  $K$  will be a real symmetric matrix. We can now rewrite (2.11) as

$$T = K + iK\rho T; \quad (2.12)$$

expanding the notation again, we find

cause we expect the three-particle resonances to appear as suitable bumps in the coefficients  $C_{LS}^J(W)$  [see Eq. (1.4)] used to fit the data. We repeat that our aim is to obtain the minimal generalization which satisfies unitarity of the scheme described in the Introduction.

With the assumed approximate form (2.14) for  $K$  we can perform certain algebraic simplifications of (2.12) reminiscent of the manipulations made by Faddeev for the three-particle Schrödinger equation. Thus  $T$  will have the form

$$T = T_1 + T_2 + T_3, \quad (2.15)$$

where

$$\begin{aligned} T_1 &= k_1 + ik_1\rho(T_1 + T_2 + T_3), \\ T_2 &= k_2 + ik_2\rho(T_1 + T_2 + T_3), \\ T_3 &= k_3 + ik_3\rho(T_1 + T_2 + T_3). \end{aligned} \quad (2.16)$$

The terms  $T_1$ ,  $T_2$ , and  $T_3$  are the contributions in which the particle pairs 23, 13, and 12, respectively, interacted last in the final state. (No corresponding decomposition is made for the initial state.) We can rearrange (2.16) to obtain

$$\begin{aligned} T_1 &= t_1 + it_1\rho(T_2 + T_3), \\ T_2 &= t_2 + it_2\rho(T_1 + T_3), \\ T_3 &= t_3 + it_3\rho(T_1 + T_2), \end{aligned} \quad (2.17)$$

where

$$t_i = (1 - ik_i\rho)^{-1}k_i \quad (2.18)$$

is a two-particle  $t$  matrix with the third particle a spectator. The corresponding picture is the same as Fig. 2 with  $k_i$  replaced by  $t_i$ . Equations (2.17) are similar in structure to the Faddeev equations for three-particle scattering, the difference being

that Eqs. (2.17) are on-shell equations while the usual Faddeev equations are off-shell equations; if the propagator  $G$  in the Faddeev equations is replaced by its imaginary part  $i\rho$  we obtain Eqs. (2.17).

For the problem in hand particles 1 and 2 are  $\pi^-$ 's, and it is a reasonable approximation to neglect the interaction of these two particles:

$$k_3 = 0, \quad t_3 = 0. \quad (2.19)$$

This implies

$$\begin{aligned} T_3 &= 0, \\ T_1 &= t_1 + it_1\rho T_2, \\ T_2 &= t_2 + it_2\rho T_1. \end{aligned} \quad (2.20)$$

In these equations  $T_1$  and  $T_2$  differ from each other only by the interchange of the two identical  $\pi^-$ 's in the final state. From Bose symmetry and Eq. (2.15) it then follows that  $T_1$  and  $T_2$  are the same function of different arguments, corresponding to the interchange of the two  $\pi^-$ 's. This is certainly true at least before the angular momentum decomposition is made; after the angular momentum decomposition,  $T_1$  and  $T_2$  are the same functions of  $L$ ,  $S$ , and  $s$  only if the decomposition of  $T_1$  is made with (23)1 coupling, i.e., with particles 2 and 3 paired into the dipion in the final state, while the decomposition of  $T_2$  is made with (13)2 coupling, i.e., particles 1 and 3 paired into the dipion in the final state. Now in the equation for  $T_1$ , Eq. (2.20), it is convenient to express  $T_1$  in the (23)1 coupling scheme and also  $t_1$ , since for the latter only particles 2 and 3 interact. If we express  $T_2$  in the (13)2 coupling scheme so as to have the same function as  $T_1$ , it is then necessary to transform this to the (23)1 coupling scheme in order to obtain a simple result for the angular momentum decomposition. Thus we need the recoupling operator which enables us to transform from (13)2 coupling to (23)1 coupling. Such recoupling problems are customary in dealing with the three-particle problem. A general treatment for relativistic particles was given by Wick.<sup>12</sup> A simplified derivation of Wick's result for the special case of interest here is given in Appendix A. If we call the recoupling operator  $\mathcal{G}_{12}$ , see Eq. (A17), we see that we can rewrite the equation for  $T_1$ , Eq. (2.20), in the form

$$T_1 = t_1 + it_1\rho \mathcal{G}_{12} T_2. \quad (2.21)$$

Here  $T_1$  and  $T_2$  are the same function of different variables. We expand the notation below. Note, however, that there is only one equation now (really one set of equations); the equation for  $T_2$  is the same as the equation for  $T_1$ . On the other hand, the operator  $\mathcal{G}_{12}$  couples together states

with different  $L, S$  and is an integral operator in the dipion energy variable  $\sqrt{s}$  as well.

In order to write out Eq. (2.21) in detail we need an expression for  $t_1$ . Before the angular momentum decomposition is made this is

$$\begin{aligned} (2\pi)^3 2\omega_1 \delta^3(\vec{p}'_1 - \vec{p}_1) \frac{8\pi\sqrt{s_1}}{q_1} \\ \times \sum_s (2S+1) e^{i\delta_s} \sin\delta_s P_S(\cos\theta), \end{aligned} \quad (2.22)$$

where the  $\delta_s$  are the phase shifts for  $\pi\pi$  scattering. Writing out the  $\delta$  function in spherical coordinates, using the spherical harmonics addition theorem for  $P_S(\cos\theta)$  ( $\theta$  is the c.m. scattering angle for particles 2 and 3), and the inverse of (1.3), one can rewrite (2.22) in the form (2.5) with

$$\begin{aligned} t_{1L'S', LS}(s'_1, s_1) \\ = \frac{(4\pi)^5}{2} \frac{W}{p_1 q_1} e^{i\delta_s} \sin\delta_s \delta_{LL'} \delta_{SS'} \delta((s'_1)^{1/2} - (s_1)^{1/2}). \end{aligned} \quad (2.23)$$

So far Eq. (2.21) has been written in a form appropriate for a three-particle  $\rightarrow$  three-particle scattering problem. However, what we want is the equations describing the decay of a state with definite quantum numbers  $JMP$ . This state is produced by some complex and unknown mechanism in the reaction  $\pi^- p \rightarrow \pi^- \pi^+ \pi^- p$ . Let us represent this production process by an initial state  $|\psi_i\rangle$ . We now multiply Eq. (2.21) on the right by  $|\psi_i\rangle$ . The product quantity  $\mathcal{S}_1 \equiv T_1 |\psi_i\rangle$  then represents the decay of the state in question. Corresponding to the inhomogeneous term in (2.21) we obtain  $\mathcal{R}_1 \equiv t_1 |\psi_i\rangle$ ; for this quantity we use one of the decay amplitudes  $\mathcal{R}_{LS}$  introduced in the Introduction, Eqs. (1.4) and (1.7). In this way we can rewrite Eq. (2.21) in the form

$$\mathcal{S}_1 = \mathcal{R}_1 + it_1\rho \mathcal{G}_{12} \mathcal{S}_2, \quad (2.24)$$

appropriate for the decay problem.

It is now time to assemble the pieces and write down an honest equation with all the indices and variables explicitly displayed. Referring to (2.7), (2.13), (2.23), (2.24), and the formulas for  $\mathcal{G}_{12}$  in Appendix A, (A14)–(A25), we find

$$\begin{aligned} \mathcal{S}_a^{J^P i}(s_1) = \delta_{ai} \mathcal{R}_i(s_1) \\ + i e^{i\delta_a} \sin\delta_a \sum_b \int_{-1}^1 d(\cos\chi_1) \mathcal{K}_{ab}(1, 2) \mathcal{S}_b^{J^P i}(s_2). \end{aligned} \quad (2.25)$$

Here the indices  $a, b, i$  stand for pairs of angular

momenta  $(L_a, S_a)$ ,  $(L_b, S_b)$ , and  $(L_i, S_i)$ . All pairs  $(L_a, S_a)$ ,  $(L_b, S_b)$  which can couple to a given state  $JP$  are coupled together. In the approximation used earlier and described in the Introduction the second term on the right-hand side of (2.25) is omitted. In this case the different states  $(L_a, S_a)$  are decoupled. This decoupling corresponds to the  $\delta_{ai}$  factor in the first term of (2.25). In the complete Eq. (2.25)  $(L_i, S_i)$  is the state which occurs before the rescattering described by the integral term. The index  $i$  enumerates the distinct states; however, for each state  $i$ , all pairs  $(L_a, S_a)$  are coupled. The iteration solution of Eq. (2.25) is represented by the picture given in Fig. 3. Each blob corresponds to a two-body interaction. The inhomogeneous term  $\delta_{ai}R_i$  is represented by the portion of the diagram to the right of the wiggly line—one interaction as specified by the Breit-Wigner form of  $\mathcal{R}_i$ . The integral term on the right-hand side of (2.25) leads to successive rescatterings of the pairs 23 and 13, the final interaction occurring in the pair 23.

Finally we must correct for the isospin of the pion. So far we have treated the pions as immutable particles, taking due account of the identity of the two  $\pi^-$ 's. This ignores the possibility of charge-exchange scattering and the production of  $\pi^0$ 's somewhere along the chain of interactions pictured in Fig. 3. To take care of these possibilities properly we must introduce isospin states. The possible isospin states for three pions and the recoupling coefficients when one transforms from (13)2 to the (23)1 coupling schemes are listed in Appendix B. The general case is fairly complicated. There are seven isospin states for three pions. Restricting ourselves to the charge state  $|- - +\rangle$  with  $T_z = -1$  eliminates the  $T=0$  state. We shall further reduce the complexity by neglecting the dipion  $I=2$  states; we note that this means we assume states with two pions having  $I=2$  are not produced in the original interaction and also that the two-body  $t$  matrix  $t=0$  for the  $I=2$  state. This

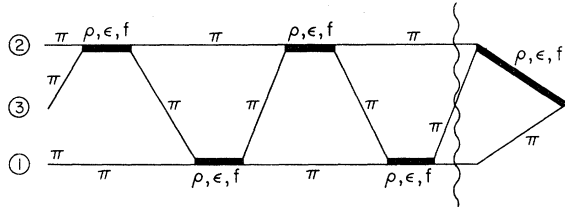


FIG. 3. The iteration solution of the integral equation (2.25) is represented by a sum of graphs of the form shown in this figure. The portion of the graph to the right of the wiggly line corresponds to the inhomogeneous term  $\delta_{ai}R_i$  in the integral equation.

leaves three states  $I=0$ ,  $T=1$  and  $I=1$ ,  $T=1$  and 2. We consider first the two coupled  $T=1$  states, with  $I=0$  and  $I=1$ . We can write down equations analogous to Eq. (2.24). We extend slightly the notation used there: In the symbol  $\mathcal{S}_i^0$  the subscript 1 means particles 2 and 3 were the last to interact; the superscript 0 means the interaction took place in the  $I=0$  state for particles 2 and 3. We have to introduce interactions in all three two-particle channels so we have six coupled amplitudes  $\mathcal{S}_1^0, \mathcal{S}_2^0, \mathcal{S}_3^0, \mathcal{S}_1^1, \mathcal{S}_2^1, \mathcal{S}_3^1$ . Let  $\mathcal{Q}_{12}$  be the angular momentum recoupling operator which transforms from channel 2 [coupling scheme (13)2] to channel 1 [coupling scheme (23)1]. Referring to the first two rows and columns of the matrix in Eq. (B2) we find as the appropriate generalization of (2.24)

$$\mathcal{S}_1^0 = \mathcal{R}_1^0 + it_1^0 \rho \left[ \frac{1}{3} \mathcal{Q}_{12} \mathcal{S}_2^0 - \frac{1}{\sqrt{3}} \mathcal{Q}_{12} \mathcal{S}_2^1 + \frac{1}{3} \mathcal{Q}_{13} \mathcal{S}_3^0 - \frac{1}{\sqrt{3}} \mathcal{Q}_{13} \mathcal{S}_3^1 \right], \quad (2.26)$$

$$\mathcal{S}_1^1 = \mathcal{R}_1^1 + it_1^1 \rho \left[ -\frac{1}{\sqrt{3}} \mathcal{Q}_{12} \mathcal{S}_2^0 + \frac{1}{2} \mathcal{Q}_{12} \mathcal{S}_2^1 + \frac{1}{\sqrt{3}} \mathcal{Q}_{13} \mathcal{S}_3^0 - \frac{1}{2} \mathcal{Q}_{13} \mathcal{S}_3^1 \right]. \quad (2.27)$$

We could write down similar equations for the pairs  $\mathcal{S}_2^0, \mathcal{S}_2^1$  and  $\mathcal{S}_3^0, \mathcal{S}_3^1$ . In order to understand the sign changes in the last two terms in Eq. (2.27) note that the order of the particles is important in Eq. (B2). If we change the order of particles 1 and 3, for example,  $|0_{13}, 1\rangle = +|0_{31}, 1\rangle$  but  $|1_{13}, 1\rangle = -|1_{31}, 1\rangle$ . In writing Eq. (2.26) we have chosen the order for the channel 3 states as  $|0_{12}, 1\rangle$  and  $|1_{12}, 1\rangle$ . We can further simplify Eqs. (2.26) and (2.27) by noting that Bose symmetry implies that  $\mathcal{S}_2^0$  and  $\mathcal{S}_2^1$  are the same functions of the coordinates of particles 1 and 3 as  $\mathcal{S}_3^0$  and  $\mathcal{S}_3^1$  are functions of the coordinates of particles 1 and 2. Also  $\mathcal{Q}_{12}$  and  $\mathcal{Q}_{13}$  are *almost* the same operators with respect to different coordinates;  $\mathcal{Q}_{12}$  transforms (13)–(23) and  $\mathcal{Q}_{13}$  transforms (12)–(23). Now for an orbital state we know that  $Y_S^{MS}(\vec{r}_3 - \vec{r}_2) = (-1)^S Y_S^{MS}(\vec{r}_2 - \vec{r}_3)$ . Thus  $\mathcal{Q}_{13}$  is the same as  $\mathcal{Q}_{12}$  except for a factor  $(-1)^S$ , where  $S$  is the dipion orbital angular momentum in the final channel containing particles 2 and 3. Keeping all this in mind we see that in the rescattering terms in Eq. (2.26), states with even  $S$  add and states with odd  $S$  cancel, whereas the reverse is true in Eq. (2.27). If we now incorporate the Pauli principle for bosons in the form which says that dipion states with  $I=0$  must have odd  $S$ , we see that we can rewrite Eqs. (2.26) and (2.27) by doubling the channel 2 contributions and dropping the channel 3 contributions:

$$\mathcal{S}_1^0 = \mathcal{R}_1^0 + it_1^0 \rho \mathcal{G}_{12} \left[ \frac{2}{3} \mathcal{S}_2^0 - \frac{2}{\sqrt{3}} \mathcal{S}_2^1 \right], \quad (2.28)$$

$$\mathcal{S}_1^1 = \mathcal{R}_1^1 + it_1^1 \rho \mathcal{G}_{12} \left[ -\frac{2}{\sqrt{3}} \mathcal{S}_2^0 + \mathcal{S}_2^1 \right]. \quad (2.29)$$

As a final step we take the projection on the charge state  $|- - + \rangle$ . This is more convenient in what follows because it is this charge state which is measured experimentally and not the isospin states. From the coefficients listed in Eqs. (B5)–(B8) we find for these projections

$$\mathcal{P}_1^0 = \frac{1}{\sqrt{3}} \mathcal{S}_1^0, \quad \mathcal{P}_2^0 = \frac{1}{\sqrt{3}} \mathcal{S}_2^0, \quad (2.30)$$

$$\mathcal{P}_1^1 = -\frac{1}{2} \mathcal{S}_1^1, \quad \mathcal{P}_2^1 = -\frac{1}{2} \mathcal{S}_2^1.$$

Substituting (2.30) in (2.28) and (2.29) we find

$$\mathcal{P}_1^0 = \mathcal{R}_1^0 + it_1^0 \rho \mathcal{G}_{12} \left[ \frac{2}{3} \mathcal{P}_2^0 + \frac{4}{3} \mathcal{P}_2^1 \right], \quad (2.31)$$

$$\mathcal{P}_1^1 = \mathcal{R}_1^1 + it_1^1 \rho \mathcal{G}_{12} \left[ \mathcal{P}_2^0 + \mathcal{P}_2^1 \right]. \quad (2.32)$$

We recall that Eqs. (2.31) and (2.32) apply to the total isospin  $T=1$  states and neglect all  $I=2$  dipion production and interactions. For the  $T=2$  state there is only one state and we find for the  $|- - + \rangle$  projection

$$\mathcal{P}_1^1 = \mathcal{R}_1^1 + it_1^1 \rho \mathcal{G}_{12} \mathcal{P}_1^1. \quad (2.33)$$

These equations are to be interpreted in the sense of Eq. (2.25); thus (2.33) is identical to (2.25), and (2.31) and (2.32) differ only in the addition of the coupling of the two isospin states. For a first attempt at using these functions to reanalyze the data we shall neglect the  $T=2$  state, Eq. (2.33). With just the  $T=1$  states, Eqs. (2.31) and (2.32), the situation is only slightly more complicated than when isospin is ignored, Eq. (2.25). In particular, when we recall that in Eqs. (2.31) and (2.32)  $I=0$  has  $S=\text{even}$  and  $I=1$  has  $S=\text{odd}$ , we see that the number of states is the same and thus also the number of parameters to be determined by fitting the experimental data.

### III. TWO-PARTICLE UNITARITY

The equations in Sec. II were set up so as to satisfy the three-particle unitarity equation (2.3). We now show that the result, Eq. (2.25), also satisfies a form of two-particle unitarity. For this purpose we rewrite (2.25) as

$$\mathcal{S}_a(s_1) = \mathcal{R}_a(s_1) + ie^{i\delta_a} \sin \delta_a \sum_b \mathcal{G}_{12} \mathcal{S}_b(s_2). \quad (3.1)$$

Now  $\mathcal{S}_a(s_1)$  is an analytic function of the dipion mass squared variable  $s_1$  with a cut starting at the two-pion threshold  $s_1 = 4m_\pi^2$ . To study the behavior near this cut it is convenient to introduce the dipion relative momentum  $q_1 = \frac{1}{2}(s_1 - 4m_\pi^2)^{1/2}$ . If

we move from the top of the cut around the end at  $s_1 = 4m_\pi^2$  to the bottom,  $q_1 \rightarrow -q_1$ . Similarly, it is well known from two-particle scattering theory that if we move from the top of the cut to the bottom,  $\delta_a \rightarrow -\delta_a$ . Near  $s_1 = 4m_\pi^2$  there is in fact a threshold dependence  $\delta_a \propto q_1^{2S_a+1}$ . Consider the inhomogeneous term  $\mathcal{R}_a(s_1)$ . Referring to Eqs. (1.7) and (1.8) and recalling that the Breit-Wigner form of (1.7) is only a convenient approximation to the energy dependence of the phase shift  $\delta_a$ , we find

$$\begin{aligned} \mathcal{R}_a(s_1) &= \frac{p_1^{L_a} q_1^{S_a}}{M_R^2 - s_1 - iM_R \Gamma} \\ &= \frac{p_1^{L_a} q_1^{S_a}}{M_R \Gamma} \sin \delta_a e^{i\delta_a}, \end{aligned} \quad (3.2)$$

where we recall that  $\Gamma \propto q_1^{2S_a+1}$ . Using the results quoted above for  $q_1$  and  $\delta_a$  we see that  $\mathcal{R}_a(s_1)$  has the special structure

$$\mathcal{R}_a(s_1) = e^{i\delta_a} q_1^{S_a} \gamma_a(s_1), \quad (3.3)$$

where  $\gamma_a(s_1)$  is an analytic function of  $s_1$  with no cut and no branch point at  $s_1 = 4m_\pi^2$ . If we move from the top of the cut around the end to the bottom  $\mathcal{R}_a(s_1)$  changes to

$$\mathcal{R}_a(s_1) \rightarrow (-1)^{S_a} e^{-i\delta_a} q_1^{S_a} \gamma_a(s_1). \quad (3.4)$$

The behavior described by (3.3) and (3.4) is of the special form required by Watson's theorem, which in turn is based on very general considerations of analyticity and unitarity.<sup>10,13</sup> We now want to point out that if the procedure for analysis described in the Introduction is used, this theorem is violated, whereas if the unitary states described in Sec. II are used the theorem is restored. To see that the scheme described in the Introduction violates the theorem, note that  $\mathcal{R}_a(s_1)$  is not the only contribution. We must also add in the recoupled transform of the same states  $\mathcal{R}_b(s_2)$  which appear due to the Bose symmetrization—see Eq. (1.4). The total contribution expressed in the (23) 1 coupling scheme is then

$$\mathcal{R}_a(s_1) + \sum_b \mathcal{G}_{12} \mathcal{R}_b(s_2). \quad (3.5)$$

As discussed above the first term here satisfies Watson's theorem. The second term does not. As we show below the second term changes by a factor  $(-1)^{S_a}$  when we move around the end of the cut; the phase factor  $e^{i\delta_a}$  is, however, missing.

Suppose, on the other hand, we use the unitary states as described in Sec. II. Then the complete contribution is the sum of  $\mathcal{S}_a(s_1)$  given by (3.1) and the recoupled transform of  $\mathcal{S}_b(s_2)$  from the other two-pion channel:

$$\begin{aligned}
\mathcal{S}_a(s_1) + \sum_b \mathcal{G}_{12} \mathcal{S}_b(s_2) \\
&= \mathcal{R}_a(s_1) + (ie^{i\delta_a} \sin\delta_a + 1) \sum_b \mathcal{G}_{12} \mathcal{S}_b(s_2) \\
&= \mathcal{R}_a(s_1) + e^{i\delta_a} \cos\delta_a \sum_b \mathcal{G}_{12} \mathcal{S}_b(s_2).
\end{aligned} \tag{3.6}$$

The second term now has the required form (3.3), provided we can show that  $\sum_b \mathcal{G}_{12} \mathcal{S}_b(s_2)$  changes only by a factor  $(-1)^{S_a}$  when we go around the end of the two-pion cut, i.e., make the change  $q_1 \rightarrow -q_1$ . This second term is an integral, given explicitly in Appendix A, (A14). Referring to Fig. 4, we see that the simultaneous changes  $q_1 \rightarrow -q_1$  and  $\chi_1 \rightarrow \chi_1 + \pi$  will have no effect on this integral since  $\chi_1$  is a dummy integration variable. Thus the change due to the replacement  $q_1 \rightarrow -q_1$  is the same as that resulting from the replacement

$$d_{v_a 0}^{S_a}(\chi_1) \rightarrow d_{v_a 0}^{S_a}(\chi_1 + \pi) = (-1)^{S_a} d_{v_a 0}^{S_a}(\chi_1), \tag{3.7}$$

as one can check from an explicit formula for  $d$  functions.<sup>14</sup> This completes the demonstration that (3.6) has the correct behavior near the two-pion cut, as required by Watson's theorem.

#### IV. CALCULATION OF UNITARIZED AMPLITUDES

Equations (2.31) and (2.32) were solved numerically for the states  $J^P = 0^-, 1^+, 2^-, 3^+$  and  $J^P = 2^+$ .

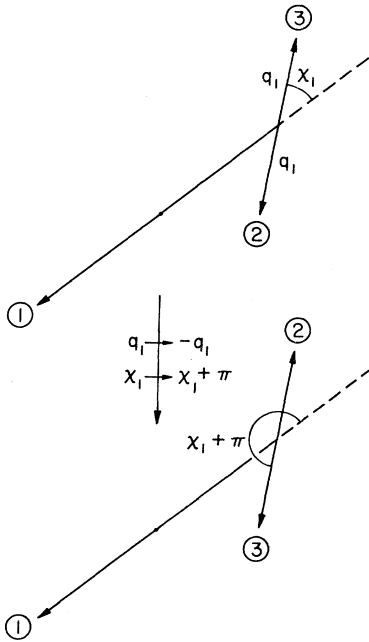


FIG. 4. Diagram to help visualize what happens under the transformations  $q_1 \rightarrow -q_1$  and  $\chi_1 \rightarrow \chi_1 + \pi$ .

For each  $J^P$ , the component states with dipion spin values  $S=0$  ( $\epsilon$ ),  $S=1$  ( $\rho$ ), and  $S=2$  ( $f$ ), together with all values of the orbital angular momentum  $L$  allowed by angular momentum and parity conservation, were used. The  $S$  and  $L$  values used for each  $J^P$  are shown in Table II.

The numerical solution of the equation was carried out, for each  $J^P$  state, at  $W=M_{3\pi}$  values of 0.86 GeV to 2.02 GeV in steps of 0.04 GeV. The values of the amplitudes (at each  $W$ ) were obtained at 25 equally spaced points in the dipion mass, from  $\sqrt{s_1} = m_{\pi\pi} = 2m_\pi$  to  $\sqrt{s_1} = W - m_\pi$ .

Numerical problems were minimized by taking into account the threshold behavior of the amplitudes at the edges of the Dalitz plot (at  $\sqrt{s_1} = 2m_\pi$ , i.e.,  $q_1 \rightarrow 0$ , and at  $\sqrt{s_1} = W - m_\pi$ , i.e.,  $p_1 \rightarrow 0$ ). Furthermore, the equations were manipulated so that the equations actually solved dealt directly with the unitarity correction terms [the second terms in Eqs. (2.31) and (2.32)], with the  $it_1 = ie^{i\delta_a} \sin\delta_a$  factor and the threshold factors removed. The accuracy of the solutions was checked by increasing the number of points from 25 to as many as 74, and by substituting the results (with interpolation as required) into the original equations.

It is worthwhile to pause and review the results obtained from these calculations before proceeding to the actual confrontation between the unitarized amplitudes and the  $3\pi$  data. Figure 5 illustrates some results. The curves shown are for the state  $J^P = 1^+$  at  $W = M_{3\pi} = 1.1$  GeV, i.e., near the center of the  $A_1$ . Each row gives the solution of the equations with one pair of  $S$  and  $L$  values for the initial state. For instance, the first row corresponds to  $S_{in} = 0$  ( $\epsilon$ ),  $L_{in} = 1$ , i.e., to the partial wave  $1^+P(\epsilon\pi)$  before rescattering. As a result of rescattering all  $J^P = 1^+$  states are present. The first column through fifth column in the figure correspond to the final state partial waves:

$$1^+P(\epsilon\pi), 1^+S(\rho\pi), 1^+D(\rho\pi), 1^+P(f\pi), 1^+F(f\pi).$$

It should be noted that the scales used are different for different amplitudes, so that some of the amplitudes are in fact quite small.

If one's attention is focused on the first two

TABLE II.  $S$  and  $L$  values included in calculation of unitarized amplitudes.

|             |       | $S=0$ ( $\epsilon$ ) | $S=1$ ( $\rho$ ) | $S=2$ ( $f$ ) |
|-------------|-------|----------------------|------------------|---------------|
| $J^P = 0^-$ | $L =$ | 0                    | 1                | 2             |
| $J^P = 1^+$ | $L =$ | 1                    | 0, 2             | 1, 3          |
| $J^P = 2^-$ | $L =$ | 2                    | 1, 3             | 0, 2, 4       |
| $J^P = 3^+$ | $L =$ | 3                    | 2, 4             | 1, 3, 5       |
| $J^P = 2^+$ | $L =$ | ...                  | 2                | 1, 3          |



rows, one notices that the most important effect is the feedthrough into the  $1^+P(\epsilon\pi)$  state from the  $1^+S(\rho\pi)$  state. This means that if one assumes a certain amount of  $1^+S(\rho\pi)$  production, the unitarity correction results in a very substantial amount of  $1^+P(\epsilon\pi)$  in the  $3\pi$  final state. The reverse effect [initial  $1^+P(\epsilon\pi)$ , final  $1^+S(\rho\pi)$ ] is not as spectacu-

lar. The partial wave  $1^+P(\epsilon\pi)$  from the initially produced  $1^+P(\epsilon\pi)$  is somewhat distorted (the real part is increased), but our experience suggests that this should make very little difference to the fits to the  $3\pi$  data. The results concerning the other unnatural parity states, especially  $0^-$ , are quite similar, i.e., the main effect is the rescat-

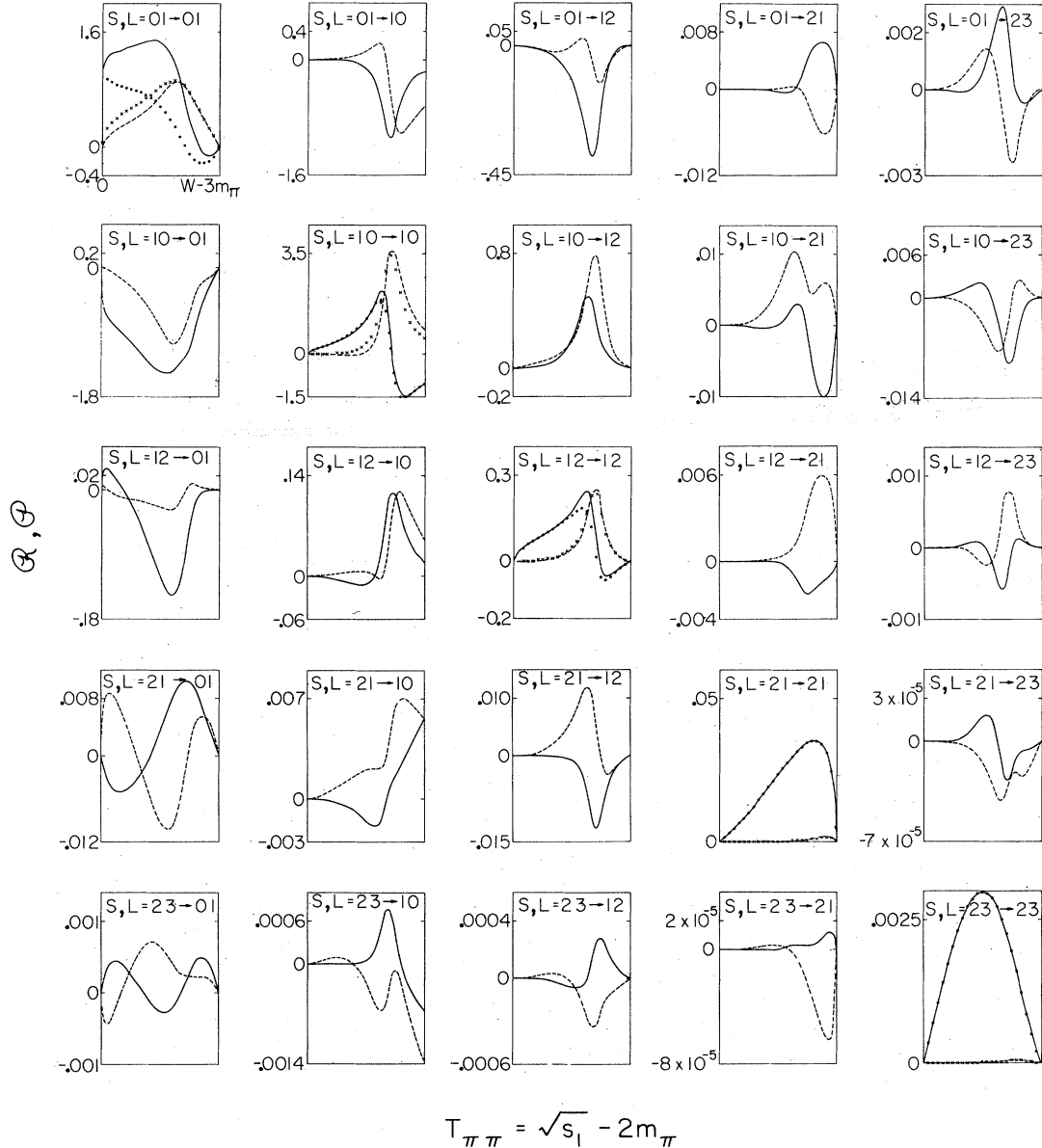


FIG. 5. The unitarized amplitudes,  $\phi$ , and nonunitarized amplitudes,  $R$ , for  $J^P=1^+$  at  $M_{3\pi}=1.1$  GeV. Rows are labeled by  $S, L$  (see text) values of the initial state; columns by the  $S, L$  values of the final state. The ordinate scales are shown so that direct comparison of amplitudes in one row is possible. Note that scales differ. The ordinate units are  $\text{GeV}^n$ ,  $n=(L+S)_{\text{in}}-2$ . The abscissa  $T_{\pi\pi}$  runs from 0 to  $W-3m_{\pi}$  in each of the 25 graphs. —  $\text{Re}(\phi)$ , ----  $\text{Im}(\phi)$ , .....  $\text{Re}(R)$ , and  $\times\times\times\times$   $\text{Im}(R)$  ( $R=0$  for off-diagonal terms).

tering from a  $\rho\pi$  initial state resulting in substantial amounts of  $\epsilon\pi$  in the final state.

Practically nothing happens to the natural parity  $2^+D$  state, since  $\epsilon\pi$  states are not allowed, and  $f\pi$  states are unimportant in the relevant mass region (near the  $A_2$  mass).

*A priori* one would certainly expect that the results of reanalyzing the  $3\pi$  data using the unitarized amplitudes could be substantially different, particularly with regard to the decomposition of the  $J^P=0^-, 1^+$ , (possibly  $2^-$ ) states into  $\rho\pi$  and  $\epsilon\pi$  partial waves. The comparison, given in Sec. V, shows that in fact the changes are rather smaller than one might have guessed.

One further point should be emphasized. As discussed in previous sections, the unitarized amplitudes satisfy unitarity conditions. Very drastic assumptions (guesses) were, however, made in the calculations, for which no theoretical or experimental basis does in fact exist. In the discussion in Sec. II, the matrix  $T$  was supposed to be the full  $3\pi \rightarrow 3\pi$  scattering matrix about which we know *nothing* except that it must satisfy the unitarity conditions [Eq. (2.12) and the additional two-body unitarity conditions discussed in Sec. III].

The key assumption, Eq. (2.14), is plausible, but could be drastically wrong. To emphasize this point we show, in Fig. 6, the ratio of the square of our unitarized amplitude for the  $2^+D$  state (integrated over all decay variables) to the corresponding quantity for the nonunitarized amplitude. It is clear that there is no sign of anything happening as one moves past the  $A_2$  pole. In other words, our  $3\pi \rightarrow 3\pi$  scattering amplitude does not include whatever forces (exchanges, intermediate states) are responsible for the  $A_2$  resonance. One is free to assume that the calculated amplitudes are

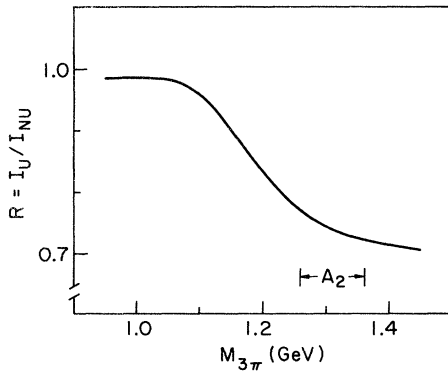


FIG. 6. The ratio  $R = I_U / I_{NU}$  vs  $M_{3\pi}$ .  $I_{NUU} = \int |\mathfrak{M}^{2^+D(\rho\pi)}|^2 d\tau$  are the integrals (over phase space) of the absolute square of the  $A_2$  amplitudes calculated from Eqs. (1.4b)–(1.8) for the NU (nonunitarized) amplitude, and from Eqs. (5.1) for the U (unitarized) amplitude.

correct in all other respects (i.e., only the  $M_{3\pi}$  dependence is wrong), but we emphasize that this is pure conjecture.

## V. COMPARISON WITH DATA

In Sec. I [see in particular Eqs. (1.2)–(1.8)] we gave the formulas assumed in fitting the data with nonunitarized amplitudes. In the unitarized formalism we replace Eq. (1.4b) by

$$\mathfrak{M}_{L'S'}^{JMP} = \sum_{L''S''} \mathcal{P}_{L''S''}^{JPL'S}(s_1) Z_{L''S''}^{JM}(\Omega_1, \bar{\Omega}_1) + (1-2). \quad (5.1)$$

Equation (5.1) corresponds to keeping, in the observed  $3\pi$  final states, “all possible” partial waves (described by the quantum numbers  $L'S'$ ). As discussed in Sec. IV, we included, in fact, only dipion spins  $S'=0, 1$ , and  $2$ .

The particular choice of the  $\pi\pi$  scattering amplitudes will, of course, affect the results. We have, in fact, used a simple Breit-Wigner description for the  $\rho$  and  $f$ , and tried two drastically different descriptions of the  $\epsilon$  (i.e., the  $S=0$  amplitude):

(a) A simple Breit-Wigner approximation with  $m_\epsilon = 0.765$  GeV,  $\Gamma_\epsilon = 0.4$  GeV, with elasticity  $\eta = 1$ .

(b) The description given by the CERN-MUNICH collaboration.<sup>15</sup> Below  $M_{3\pi} = 1.4$  GeV the two choices for the  $\epsilon$  turned out to be indistinguishable.

Although other, more complicated hypotheses were also tried, we will present here only a comparison of the results obtained using a rather simple hypothesis in which the following partial waves are included:

$$\begin{aligned} &0^-S(\epsilon\pi), \quad 0^-P(\rho\pi) \\ &1^+P(\epsilon\pi), \quad 1^+S(\rho\pi), \quad J_z = 0 \text{ only} \\ &2^-P(\rho\pi), \quad J_z = 0 \text{ only} \\ &2^+D(\rho\pi), \quad J_z = \pm 1 \text{ only (in the “natural parity exchange” combination } |2^+1\rangle + |2^+-1\rangle). \end{aligned}$$

At the risk of being repetitive, we note that the above is a list of input states; for the case of unitarized amplitudes, all partial waves listed in Table II for the states  $0^-, 1^+, 2^-, 2^+$  are included in the final state.

In a preliminary account of this work<sup>11</sup> we presented the reanalysis of the combined 11–25 GeV data described in Ref. 5. Here we present the reanalysis of the larger data sample from the Serpukhov experiment (Refs. 8 and 9).

We summarize briefly the results, comparing the nonunitarized and unitarized fits to the same data sample.

(a) When the unitarized amplitudes are used to fit the data, the fits are significantly worse. This is illustrated in Fig. 7, which shows the difference in  $\chi^2$  for the unitarized and nonunitarized fits. We

have verified (by generating Monte Carlo events corresponding to the unitarized and nonunitarized fits—in the region  $M_{3\pi} = 1.2\text{--}1.4$  GeV) that this is a real effect. One can account for the decrease in likelihood by comparing Dalitz-plot distributions and moments of angular distributions for the Monte Carlo events and for the data. We remark (but omit details) that the inferiority of the U (unitarized) fits relative to the NU (nonunitarized) fits persists when more complicated hypotheses (more partial waves) are used.

(b) The amount of production of various  $J^P$  states is essentially unchanged. There is a slight decrease in the  $J^P = 1^+$  total and a slight increase in the  $J^P = 0^-$  total in going from the NU fit to the U fit—see Figs. 8 and 9. The  $J^P = 2^+$  and  $J^P = 2^-$  contributions are almost identical (Fig. 10).

(c) For the states  $J^P = 0^-$  [Figs. 8(a) and 8(b)] and  $J^P = 1^+$  [Figs. 9(a) and 9(b)], the decomposition into  $\epsilon\pi$  and  $\rho\pi$  waves is different for the two fits. For  $J^P = 0^-$  [Figs. 8(a) and 8(b)] the number of events ascribed to both  $0^-S(\epsilon\pi)$  and  $0^-P(\rho\pi)$  by the U fit is larger. The excess events are canceled by a strong negative interference between the two waves. Exactly the same remarks can be applied to describe the  $J^P = 1^+$  results [Figs. 9(a) and 9(b)]. Again the U fits give more  $1^+P(\epsilon\pi)$ , more  $1^+S(\rho\pi)$ , and a strong negative interference.

It is quite clear what the data are telling us: The rescattering from  $\rho\pi$  to  $\epsilon\pi$  produces more  $\epsilon\pi$  in the final state than there is  $\epsilon\pi$  in the data. The fitting procedure then includes an excess of direct  $\epsilon\pi$  production amplitude and cleverly adjusts the relative phases to cancel (as much as possible of) the unitarity

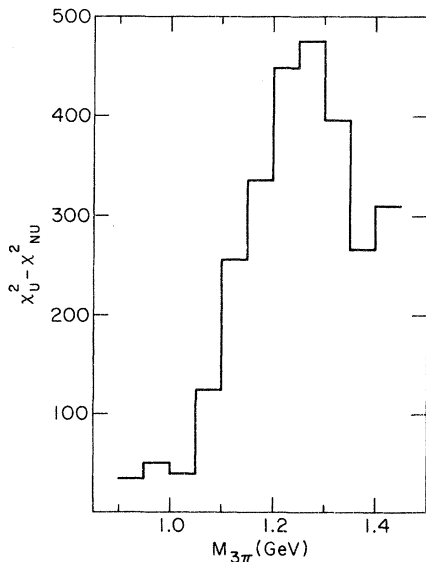


FIG. 7.  $\chi^2$  difference between U (unitarized) and NU (nonunitarized) fits to the Serpukhov data (Refs. 8 and 9).

correction terms. One is strongly tempted to conclude that the rescattering corrections obtained with our unitarization procedure are too large. The correct amplitudes, which must, of course, be unitary, nevertheless appear to be better approximated by ignoring the rescattering corrections altogether (NU fits) than by our present attempts at unitarization.

(d) In spite of our strong reservations about the correctness of our rescattering correction, we show (Fig. 11) what happens to the phases of the  $A_1 [J^P = 1^+S(\rho\pi)]$  wave relative to other waves. We would comment that

(d1) the  $M_{3\pi}$  dependence of the relative phases is essentially the same for the U and NU fits, although the phases themselves have been shifted.

(d2) In both U and NU fits the  $1^+S(\rho\pi)$  relative phases show little sign of change in the region  $M_{3\pi} = 1.0\text{--}1.4$  GeV. This behavior is to be contrasted with the normal Breit-Wigner variation

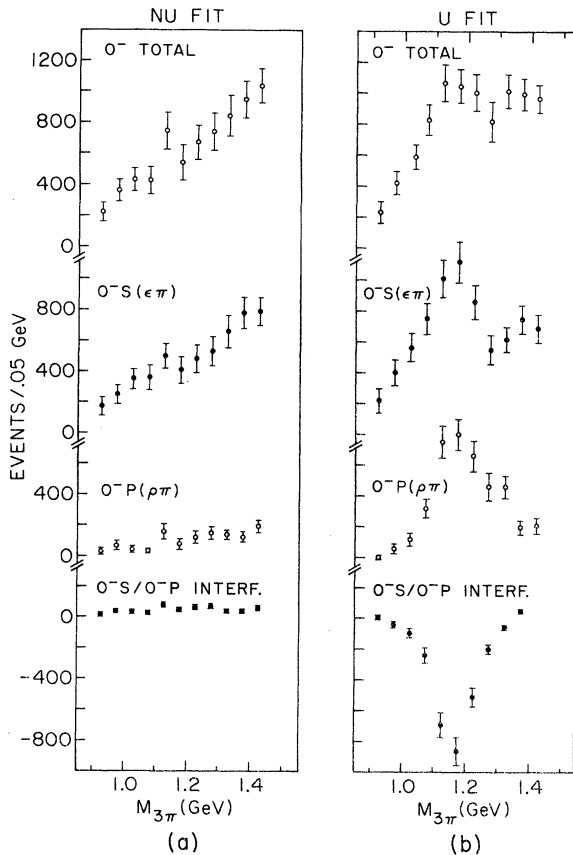


FIG. 8. Comparison of NU (nonunitarized) and U (unitarized) fits to the Serpukhov data (Refs. 8 and 9). The number of events per 0.05 GeV is shown for total  $J^P = 0^-$ ,  $0^-S(\epsilon\pi)$ ,  $0^-P(\rho\pi)$ , and  $0^-S\text{--}0^-P$  interference. (a) nonunitarized fits and (b) unitarized fits.

of phase obtained for the  $A_2 [J^P = 2^+ D(\rho\pi)]$  state in both U and NU fits (fig. 12).

In summary, our unitarized functions are a disappointment. Although properly unitary, they appear to be a less suitable set of functions in terms of which to describe the data than the simple non-unitarized functions. If nevertheless we use them to fit the data, we find, just as in the original non-unitary analysis,<sup>9</sup> no evidence for a resonant variation of the  $A_1 [J^P = 1^+ S(\rho\pi)]$  phase.

*Note Added.* It has been called to the authors' attention that the relativistic minimal  $K$ -matrix formalism used in this paper was set up in an earlier paper by K. L. Kowalski.<sup>16</sup>

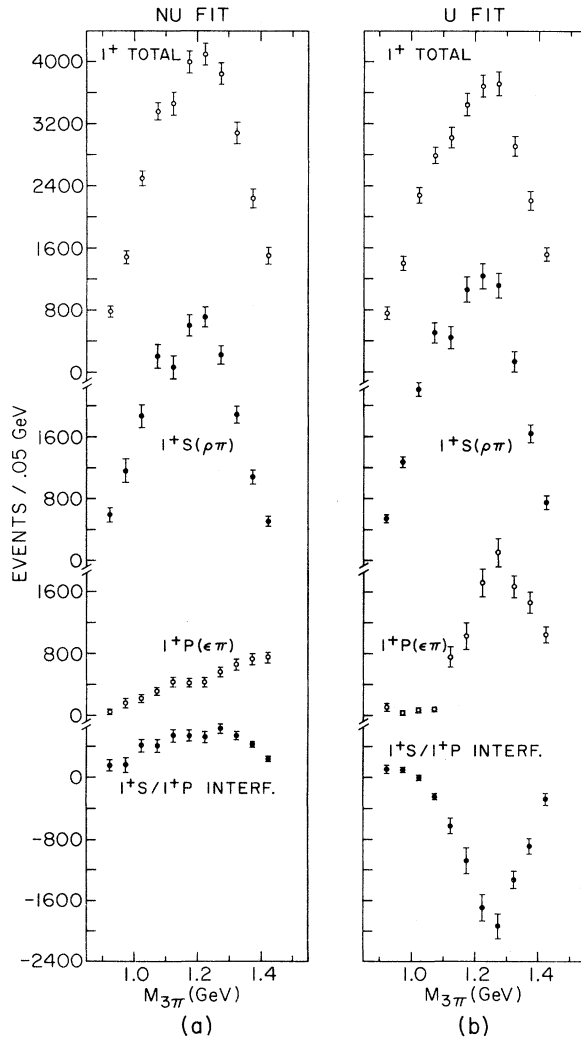


FIG. 9. Comparison of NU (nonunitarized) and U (unitarized) fits to the Serpukhov data (Refs. 8 and 9). The number of events per 0.05 GeV is shown for total  $J^P = 1^+$ ,  $1^+ S(\rho\pi)$ ,  $1^+ P(\epsilon\pi)$ , and  $1^+ S-1^+ P$  interference. (a) nonunitarized fits and (b) unitarized fits.

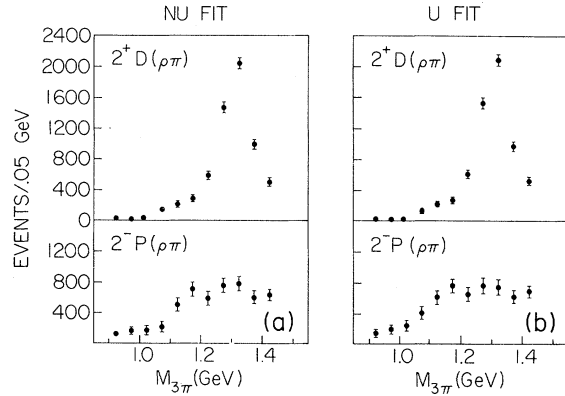


FIG. 10. Comparison of NU (nonunitarized) and U (unitarized) fits to the Serpukhov data (Refs. 8 and 9). The number of events per 0.05 GeV is shown for  $2^+ P(\rho\pi)$  and  $2^+ D(\rho\pi)$ . (a) nonunitarized fits and (b) unitarized fits.

#### ACKNOWLEDGMENTS

We are much indebted to Roy Schult for help with the theory of the three-particle problem and to Robert Klanner for help with the data tape of the Serpukhov data.

#### APPENDIX A

We give in this appendix what we hope is a short and simple derivation of the angular momentum recoupling operator necessary when one wishes to transform from the (13)2 coupling scheme in which particles 1 and 3 are paired as a dipion to the (23)1 coupling scheme in which particles 2 and 3 are paired as a dipion. The general case has been treated by Wick.<sup>11</sup> We restrict ourselves here to the case of three spinless particles of equal

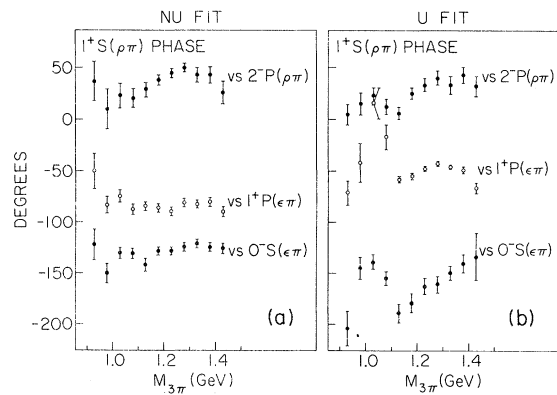


FIG. 11. Comparison of NU (nonunitarized) and U (unitarized) fits to the Serpukhov data (Refs. 8 and 9). The phase of  $1^+ S(\rho\pi)$  relative to  $0^- S(\epsilon\pi)$ ,  $1^+ P(\epsilon\pi)$ , and  $2^- P(\rho\pi)$  is shown. (a) nonunitarized fits and (b) unitarized fits.

mass (three pions). The kinematics is treated relativistically.

It is convenient to introduce both helicity amplitudes and  $LS$  amplitudes. The wave function  $\psi_{JMP}$  of a three-pion state with quantum numbers  $JMP$  can be expressed in terms of helicity amplitudes  $f_{\mu}^{JP}$  as

$$\psi_{JMP} = \sum_{\mu} \left( \frac{2J+1}{8\pi^2} \right)^{1/2} D_{M\mu}^{J*}(R_1) f_{\mu}^{JP1}(s_1, s_2). \quad (\text{A1})$$

Here  $s_1, s_2$  are Dalitz-plot variables,  $D_{M\mu}^J$  is a Wigner  $D$  function, and  $R_1$  stands for Euler angles  $\alpha_1, \beta_1, \gamma_1$  describing the rotation which carries the three-pion system with fixed  $s_1, s_2$  from a standard configuration to the actual configuration. The standard configuration is arbitrary. We use the following conventions: The superscript 1 on  $f_{\mu}^{JP1}$  and the subscript on  $R_1$  indicate that in this standard configuration particle 1 is moving in the  $-z$  direction and particle 3 is moving in the  $xz$  plane with a positive  $x$  component of its momentum—see Fig. 13(a). We also have

$$\psi_{JMP} = \sum_{\nu} \left( \frac{2J+1}{8\pi^2} \right)^{1/2} D_{M\nu}^{J*}(R_2) f_{\nu}^{JP2}(s_1, s_2), \quad (\text{A2})$$

where now the standard configuration is chosen differently. The subscript and superscript 2 indicate that in this standard configuration particle 2 is moving along the  $-z$  direction and particle 3 is moving in the  $xz$  plane with a positive  $x$  component of its momentum—see Fig. 13(b). Since the actual configuration of the system is the same in both cases we have a relation between the rotation group elements  $R_1$  and  $R_2$ ,

$$R_2 = R_1 r_{12}, \quad (\text{A3})$$

where  $r_{12}$  is the rotation which carries the standard configuration 2 into the standard configura-

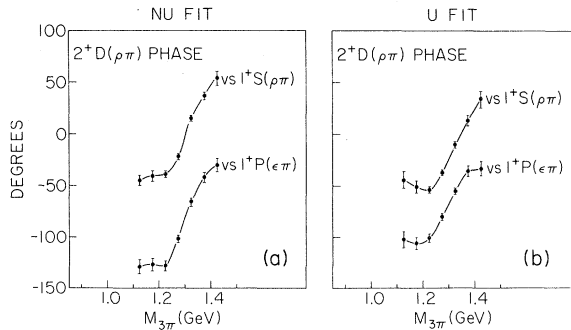


FIG. 12. Comparison of NU (nonunitarized) and U (unitarized) fits to the Serpukhov data (Refs. 8 and 9). The phase of  $2^+D(\rho\pi)$  relative to  $1^+S(\rho\pi)$  and  $1^+P(\epsilon\pi)$  is shown. (a) nonunitarized fits and (b) unitarized fits. Curves are drawn to guide the eye.

tion 1. Using simple properties of the representation  $D_{M\mu}^J$  of the rotation group, we find from the equality of (A1) and (A2)

$$\begin{aligned} \sum_{\nu} D_{M\nu}^{J*}(R_1) f_{\nu}^{JP1} &= \sum_{\mu} D_{M\mu}^{J*}(R_1 r_{12}) f_{\mu}^{JP2} \\ &= \sum_{\mu, \nu} D_{M\nu}^{J*}(R_1) D_{\nu\mu}^{J*}(r_{12}) f_{\mu}^{JP2}. \end{aligned} \quad (\text{A4})$$

From the orthonormality of the  $D_{M\nu}^J(R)$  we then obtain

$$f_{\nu}^{JP1} = \sum_{\mu} D_{\nu\mu}^{J*}(r_{12}) f_{\mu}^{JP2}. \quad (\text{A5})$$

A glance at Fig. 13 shows that  $r_{12}$  is a rotation through  $180^\circ$  about the  $z$  axis followed by a rotation through a positive angle  $\theta_{12}$  about the  $y$  axis. From the standard formulas for  $D$  functions we then find

$$D_{\nu\mu}^{J*}(r_{12}) = (-1)^\mu d_{\nu\mu}^J(\theta_{12}). \quad (\text{A6})$$

We can now relate the two sets of helicity amplitudes discussed above to the two sets of  $LS$  amplitudes corresponding to the two coupling schemes (23)1 and (13)2. If we call the  $LS$  amplitude for the coupling scheme (23)1  $F_{LS}^{J1}(s_1)$ , we can write the state  $\psi_{JMP}$  in the (23)1  $LS$  coupling scheme as

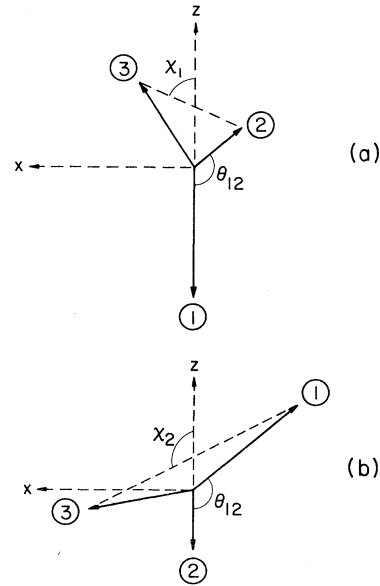


FIG. 13. The orientations of the particles in the standard configurations 1 and 2 correspond to parts (a) and (b) of the figure.

$$\psi_{JMP} = \sum_{L,S} F_{LS}^{J_1}(s_1) \sum_{\mu} \langle JM | LSm\mu \rangle \left( \frac{2L+1}{4\pi} \right)^{1/2} D_{m0}^{L*}(\varphi_1, \theta_1, 0) \left( \frac{2S+1}{4\pi} \right)^{1/2} D_{\mu 0}^{S*}(\bar{\varphi}_1, \bar{\theta}_1, 0). \quad (\text{A7})$$

The angles used in this formula are defined in Fig. 1. For comparison with Eq. (1.3) we remind the reader that  $[(2l+1)/4\pi]^{1/2} D_{m0}^{l*}(\varphi, \theta, 0)$  is a normalized spherical harmonic  $Y_l^m(\theta, \varphi)$ . In order to obtain the relation between  $f_{\mu}^{JP_1}$  and  $F_{LS}^{J_1}$  compare (A1) and (A7) in the limit when the rotation  $R_1 = (\alpha, \beta, \gamma) = 1$  is no rotation at all. In this limit  $D_{M\mu}^J(R_1) = \delta_{M\mu}$ ,  $\theta_1 = 0$ ,  $D_{m0}^{L*}(\varphi_1, \theta_1, 0) = \delta_{m0}$ ,  $\bar{\varphi}_1 = 0$ ,  $\bar{\theta}_1 = \chi_1$ . The angle  $\chi_1$  is indicated in Fig. 13(a); it is measured in the 23 center-of-mass system; a formula for it appears below. Making these substitutions we find

$$f_{\mu}^{JP_1}(s_1, s_2) = \sum_{L,S} F_{LS}^{J_1}(s_1) \left( \frac{2L+1}{2J+1} \right)^{1/2} \langle J\mu | LS0\mu \rangle \times \left( \frac{2S+1}{2} \right)^{1/2} d_{\mu 0}^S(\chi_1). \quad (\text{A8})$$

In exactly the same way we obtain

$$f_{\mu}^{JP_2}(s_1, s_2) = \sum_{L,S} F_{LS}^{J_2}(s_2) \left( \frac{2L+1}{2J+1} \right)^{1/2} \langle J\mu | LS0\mu \rangle \times \left( \frac{2S+1}{2} \right)^{1/2} d_{\mu 0}^S(\chi_2). \quad (\text{A9})$$

The angle  $\chi_2$  is indicated in Fig. 13(b); it is measured in the 13 center-of-mass system.

We can now combine (A5), (A8), and (A9) to find the relation between  $F_{LS}^{J_1}(s_1)$  and  $F_{LS}^{J_2}(s_2)$ . Using the orthogonality properties of the  $d_{\mu 0}^S$  functions, we obtain from (A8)

$$\left( \frac{2S_a+1}{2} \right)^{1/2} \int_{-1}^{+1} d(\cos\chi_1) f_{\nu_a}^{JP_1}(s_1, s_2) d_{\nu_a 0}^{S_a}(\chi_1) = \sum_L F_{LS_a}^{J_1}(s_1) \left( \frac{2L+1}{2J+1} \right)^{1/2} \langle J\nu_a | LS_a 0\nu_a \rangle. \quad (\text{A10})$$

Using standard transformation formulas for Clebsch-Gordan coefficients we find

$$\left( \frac{2l+1}{2j+1} \right)^{1/2} \langle j\nu | ls0\nu \rangle = (-1)^{s+\nu} \langle l0 | js-\nu\nu \rangle, \quad (\text{A11})$$

and hence from the unitarity of the Clebsch-Gordan coefficients,

$$\sum_{\nu} \left( \frac{2l+1}{2j+1} \right)^{1/2} \langle j\nu | ls0\nu \rangle \left( \frac{2l'+1}{2j'+1} \right)^{1/2} \langle j\nu | l's0\nu \rangle = \delta_{ll'}. \quad (\text{A12})$$

With this we can complete the inversion of (A10):

$$F_{L_a S_a}^{J_1}(s_1) = \left[ \frac{(2L_a+1)(2S_a+1)}{2(2J+1)} \right]^{1/2} \times \sum_{\nu_a} \langle J\nu_a | L_a S_a 0\nu_a \rangle \times \int_{-1}^1 d(\cos\chi_1) d_{\nu_a 0}^{S_a}(\chi_1) f_{\nu_a}^{JP_1}(s_1, s_2). \quad (\text{A13})$$

Substituting (A5), (A6), and (A9) in (A13), we finally obtain

$$F_{L_a S_a}^{J_1}(s_1) = \sum_{L_b S_b} \int_{-1}^1 d(\cos\chi_1) \mathcal{K}_{ab}(1, 2) F_{L_b S_b}^{J_2}(s_2), \quad (\text{A14})$$

where

$$\mathcal{K}_{ab}(1, 2) = \sum_{\nu_a \nu_b} C(J, L_a, S_a, \nu_a) C(J, L_b, S_b, \nu_b) (-1)^{\nu_b} \times d_{\nu_a 0}^{S_a}(\chi_1) d_{\nu_a \nu_b}^J(\theta_{12}) d_{\nu_b 0}^{S_b}(\chi_2), \quad (\text{A15})$$

and

$$C(J, L, S, \nu) = \left[ \frac{(2L+1)(2S+1)}{2(2J+1)} \right]^{1/2} \langle J\nu | LS0\nu \rangle. \quad (\text{A16})$$

In Eq. (2.21) of the main text of this paper we have compressed the notation to the extent of expressing the transformation (A14), (A15), and (A16) by

$$F^1 = \mathcal{G}_{12} F^2. \quad (\text{A17})$$

It remains to specify the kinematical relations in detail. These are illustrated in Fig. 14. The angle  $\theta_{12}$  is measured in the over-all center-of-mass system of the three particles. The angle  $\chi_1$  is measured in the center-of-mass system of

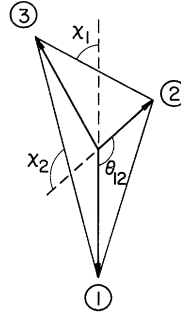


FIG. 14. Pictorial representation of the kinematic quantities employed in Eqs. (A14)–(A25).

particles 2 and 3. The angle  $\chi_2$  is measured in the center-of-mass system of particles 1 and 3. In the expression (A14)  $s_1 = (p_2 + p_3)^2$  is the square of the 23 invariant mass and  $\cos\chi_1$  is the integration variable. In terms of these  $s_2 = (p_1 + p_3)^2$  is given by

$$s_2 = \frac{1}{2}(W^2 + 3m_\pi^2 - s_1) + 2p_1q_1 \frac{W}{\sqrt{s_1}} \cos\chi_1, \quad (\text{A18})$$

where  $W^2 = (p_1 + p_2 + p_3)^2$  is the square of the three-pion invariant mass, and  $q_1$  and  $p_1$  are given by

$$q_1 = \frac{1}{2}(s_1 - 4m_\pi^2)^{1/2}, \quad (\text{A19})$$

$$p_1 = \frac{1}{2W} \{[(W - m_\pi)^2 - s_1][(W + m_\pi)^2 - s_1]\}^{1/2}. \quad (\text{A20})$$

Given  $s_1$  and  $s_2$ ,  $\cos\chi_2$  is determined by

$$\cos\chi_2 = \frac{s_1 - s_3}{4p_2q_2W/\sqrt{s_2}}, \quad (\text{A21})$$

where  $s_3$ ,  $q_2$ , and  $p_2$  are given by

$$s_3 = W^2 + 3m_\pi^2 - s_1 - s_2, \quad (\text{A22})$$

$$q_2 = \frac{1}{2}(s_2 - 4m_\pi^2)^{1/2}, \quad (\text{A23})$$

$$p_2 = \frac{1}{2W} \{[(W - m_\pi)^2 - s_2][(W + m_\pi)^2 - s_2]\}^{1/2}. \quad (\text{A24})$$

Finally  $\cos\theta_{12}$  is given in terms of previously defined quantities by

$$\cos\theta_{12} = \frac{1}{p_2} \left[ \left(1 + \frac{p_1^2}{s_1}\right)^{1/2} q_1 \cos\chi_1 - \frac{p_1}{2} \right]. \quad (\text{A25})$$

## APPENDIX B

This appendix is devoted to the recoupling problem for the isospin states for three pions. This can be handled with the apparatus of Racah coefficients. It is just as easy to use elementary methods for the few special cases of interest. For two pions the isospin can be

$$I=0 \quad 1 \quad 2.$$

Adding the isospin of a third pion to obtain total isospin, we obtain

$$T=1 \quad 0, 1, 2 \quad 1, 2, 3.$$

These seven states can be obtained either in the (23)1 coupling scheme, i.e., first couple the isospins of particles 2 and 3, then add in the isospin of particle 1, or in the (13)2 scheme in which one first couples the isospins of particles 1 and 3. For a case such as  $T=1$ , where there are three distinct states, the three states obtained in

the (13)2 coupling scheme will be linear combinations of the three states obtained in the (23)1 scheme. We can use state symbols such as  $|I_{13}, T\rangle$  to mean that the isospins of particles 1 and 3 are combined to obtain an isospin  $I$  state, which is then combined with the isospin of particle 2 to obtain a total isospin  $T$  state. With this notation we find for the recoupling coefficients

$$|1_{13}, 0\rangle = -|1_{23}, 0\rangle, \quad (\text{B1})$$

$$\begin{bmatrix} |0_{13}, 1\rangle \\ |1_{13}, 1\rangle \\ |2_{13}, 1\rangle \end{bmatrix} = \begin{bmatrix} \frac{1}{3} & -\frac{1}{\sqrt{3}} & \frac{\sqrt{5}}{3} \\ -\frac{1}{\sqrt{3}} & \frac{1}{2} & \frac{\sqrt{15}}{6} \\ \frac{\sqrt{5}}{3} & \frac{\sqrt{15}}{6} & \frac{1}{6} \end{bmatrix} \begin{bmatrix} |0_{23}, 1\rangle \\ |1_{23}, 1\rangle \\ |2_{23}, 1\rangle \end{bmatrix}, \quad (\text{B2})$$

$$\begin{bmatrix} |1_{13}, 2\rangle \\ |2_{13}, 2\rangle \end{bmatrix} = \begin{bmatrix} \frac{1}{2} & -\frac{\sqrt{3}}{2} \\ -\frac{\sqrt{3}}{2} & -\frac{1}{2} \end{bmatrix} \begin{bmatrix} |1_{23}, 2\rangle \\ |2_{23}, 2\rangle \end{bmatrix}, \quad (\text{B3})$$

$$|2_{13}, 3\rangle = |2_{23}, 3\rangle. \quad (\text{B4})$$

It is worthwhile noting that the phases of some of these coefficients are determined by the order. We have chosen the order as follows: In  $|I_{13}, T\rangle$  particles 1 and 3 are coupled first, particle 1 being the *first* and particle 3 the *second* particle; the dipion of isospin  $I$  is then coupled to the other pion, the dipion being the *first* and the other pion the *second* particle.

One way to obtain the above coefficients is to calculate overlaps between the different states expressed in terms of charge states for the 3 pions. Using a table of Clebsch-Gordan coefficients it is easy to find for the projection  $T_z = -1$

$$|0_{13}, 1\rangle = \frac{1}{\sqrt{3}} |+-\rangle - \frac{1}{\sqrt{3}} |0-0\rangle + \frac{1}{\sqrt{3}} |--\rangle, \quad (\text{B5})$$

$$|1_{13}, 1\rangle = \frac{1}{2} |+-\rangle - \frac{1}{2} |--\rangle - \frac{1}{2} |00-\rangle + \frac{1}{2} |-00\rangle, \quad (\text{B6})$$

where the symbol  $|+-\rangle$  indicates the charges of pions 1, 2, 3 in that order. Interchanging particles 1 and 2, we obtain

$$|0_{23}, 1\rangle = \frac{1}{\sqrt{3}} |-+\rangle - \frac{1}{\sqrt{3}} |-00\rangle + \frac{1}{\sqrt{3}} |--\rangle, \quad (\text{B7})$$

$$|1_{23}, 1\rangle = \frac{1}{2} |+-\rangle - \frac{1}{2} |--\rangle + \frac{1}{2} |00-\rangle + \frac{1}{2} |0-0\rangle .$$

(B8)

Taking appropriate scalar products, one imme-

diately obtains the first two rows and columns of the matrix in (B2).

\*Work supported in part by the USAEC under Contract No. AT(11-1)-1195.

†Work supported in part by NSF Grant No. GP 40908X.

<sup>1</sup>D. Brockway, thesis, University of Illinois report No. COO-1195-197, 1970 (unpublished).

<sup>2</sup>Yu. M. Antipov *et al.*, in *Experimental Meson Spectroscopy—1972*, Philadelphia, 1972, edited by Kwan-Wu Lai and Arthur H. Rosenfeld (A.I.P., New York, 1972), p. 164.

<sup>3</sup>Illinois-GHMS-H-ABCCCH-ND-W and CIBS Collaboration, *Experimental Meson Spectroscopy—1972*, Philadelphia, 1972, edited by Kwan-Wu Lai and Arthur H. Rosenfeld (A.I.P., New York, 1972), p. 185.

<sup>4</sup>G. Ascoli *et al.*, University of Illinois Report No. COO-1195-295 (unpublished); also *Phys. Rev. Lett.* **25**, 962 (1970).

<sup>5</sup>G. Ascoli *et al.*, *Phys. Rev. D* **7**, 669 (1973).

<sup>6</sup>G. Ascoli, in *Proceedings of the XVI International Conference on High Energy Physics, Chicago-Batavia, Ill., 1972*, edited by J. D. Jackson and A. Roberts (NAL, Batavia, Ill., 1973), Vol. 1, p. 3.

<sup>7</sup>R. Klanner, CERN-NP Internal Report No. 73-9 (unpublished) and Ph.D. thesis, University of Munich, 1973 (unpublished).

<sup>8</sup>Yu. M. Antipov *et al.*, *Nucl. Phys.* **B63**, 141 (1973).

<sup>9</sup>Yu. M. Antipov *et al.*, *Nucl. Phys.* **B63**, 153 (1973).

<sup>10</sup>G. Fox, in *Experimental Meson Spectroscopy—1972*, Philadelphia, 1972, edited by Kwan-Wu Lai and Arthur H. Rosenfeld (A.I.P., New York, 1972), p. 271.

<sup>11</sup>G. Ascoli and H. W. Wyld, in *Experimental Meson Spectroscopy—1974*, Boston, 1974, edited by D. A. Garelick (A.I.P., New York, 1974), p. 59. See also the account of similar work by Y. Goradia, T. Lasinski, H. Tabak, and G. Smadja, paper submitted to the Conference on Experimental Meson Spectroscopy, Boston 1974 (unpublished).

<sup>12</sup>G. C. Wick, *Ann. Phys. (N.Y.)* **18**, 65 (1962).

<sup>13</sup>K. W. Watson, *Phys. Rev.* **88**, 1163 (1952); R. J. Eden, P. V. Landshoff, D. I. Olive, J. C. Polkinghorne, *The Analytic S-Matrix* (Cambridge Univ. Press, Cambridge, England, 1966), p. 232; D. J. Olive, *Nuovo Cimento* **37**, 1422 (1965); D. A. Jacobson, *ibid.* **51**, 624 (1967); P. R. Graves-Morris, *ibid.* **54**, 817 (1968).

<sup>14</sup>M. E. Rose, *Elementary Theory of Angular Momentum* (Wiley, New York, 1957), p. 52.

<sup>15</sup>B. Hyams *et al.*, *Nucl. Phys.* **B64**, 134 (1973).

<sup>16</sup>K. L. Kowalski, *Phys. Rev. D* **7**, 2957 (1973).